The application of frequency-domain Fluorescence Lifetime Imaging Microscopy as a quantitative analytical tool for microfluidic devices

A. D. Elder[1], S. M. Matthews[1], J. Swartling[1], K. Yunus[1], J. H. Frank[2], C. M. Brennan[3], A. C. Fisher[1], and C. F. Kaminski[1]

[1]*Department of Chemical Engineering, University of Cambridge, New Museums Site, Pembroke Street, Cambridge, CB2 3RA, UK*

[2]*Sandia National Laboratories, P.O. Box 969 MS 9051, Livermore, CA 94551-0969*

[3]*Syngenta Ltd, Huddersfield Manufacturing Centre, PO Box A38, Leeds Road, Huddersfield, HD2 1FF*

cfk23@cam.ac.uk, acf42@cam.ac.uk

Abstract: We describe the application of wide-field frequency domain Fluorescence Lifetime Imaging Microscopy (FLIM) to imaging in microfluidic devices. FLIM is performed using low cost, intensity modulated Light Emitting Diodes (LEDs) for illumination. The use of lifetime imaging for quantitative analysis within such devices is demonstrated by mapping the molecular diffusion of iodide ions across a microchannel.

OCIS codes: (180.2520) Fluorescence microscopy; (170.3650) Lifetime-based sensing; (230.3670) Light-emitting diodes.

References

1. D.J. Beebe, G.A. Mensing and G.M. Walker, "Physics and Applications of Microfluidics in Biology," Annu. Rev. Biomed. Eng. **4,** 261-286 (2002).
2. S.C. Jakeway, A.J. de Mello and E.L. Russell, "Miniaturized total analysis systems for biological analysis," Fresenius J. Anal. Chem. **366,** 525-539 (2000).
3. T. Chovan and A. Guttman, "Microfabricated devices in biotechnology and biochemical processing," Trends Biotechnol. **20,** 116-122 (2002).
4. A.J. Tüd˝os, G.A.J. Besselink and R.B.M. Schasfoort, "Trends in miniaturized total analysis systems for point-of-care testing in clinical chemistry," Lab. Chip **1,** 83-96 (2001).
5. E. Verpoorte, "Microfluidic chips for clinical and forensic analysis," Electrophoresis 23, 677-712 (2002).
6. Y. Huang, E.L. Mather, J.L. Bell and M. Madou, "MEMS-based sample preparation for molecular diagnostics," Anal. Bioanal. Chem. **372,** 49-65 (2002).
7. T. Vo-Dinh and B. Cullum, "Biosensors and biochips: advances in biological and medical diagnostics," Fresenius J. Anal. Chem. **366,** 540-551 (2000).
8. Y. Sato, G. Irisawa, M. Ishizuka, K. Hishida and M. Maeda, "Visualization of convective mixing in microchannel by fluorescence imaging," Meas. Sci. Technol. **14,** 114-122 (2003).
9. R.H. Liu, M.A. Stremler, K.V. Sharp, M.G. Olsen, J.G. Santiago, R.J. Adrian, H. Aref and D.J. Beebe, "Passive mixing in a three-dimensional serpentine microchannel," J. Microelectromech. Syst. **9,** 190-197 (2000).
10. R.F. Ismagilov, A.D. Stroock, P.J.A. Kenis, G. Whitesides and H.A. Stone, "Experimental and theoretical scaling laws for transverse diffusive broadening in two-phase laminar flows in microchannels," Appl. Phys. Lett. **76,** 2376-2378 (2000).
11. C. Xi, D.L. Marks, D.S. Parikh, L. Raskin and S.A Boppart, "Structural and functional imaging of 3D microfluidic mixers using optical coherence tomography," P. Natl. Acad. Sci. USA **101,** 7516-7521 (2004).
12. R.K.P. Benninger, O. Hofmann, J. McGinty, J. Requejo-Isidro, I. Munro, M.A.A. Neil, A.J. deMello and P.M.W. French, "Time-resolved fluorescence imaging of solvent interactions in microfluidic devices," Opt. Express **13,** 6275-6285 (2005).
13. S.W. Magennis, E.M. Graham and A.C. Jones, "Quantitative Spatial Mapping of Mixing in Microfluidic Systems," Angewandte Chemie International Edition **44,** 6512-6516 (2005).
14. J. R. Lakowicz and K. W. Berndt, "Lifetime-Selective Fluorescence Imaging Using An Rf Phase- Sensitive Camera," Rev. Sci. Instrum. **62,** 1727-1734 (1991).

#69207 - $15.00 USD Received 7 April 2006; revised 26 May 2006; accepted 26 May 2006

15. G. Marriott, R.M. Clegg, D.J. Arndt-Jovin and T.M. Jovin, “Time resolved imaging microscopy. Phosphorescence and delayed fluorescence imaging,” Biophys. J. **60,** 1374-1387 (1991).
16. Q. S. Hanley and A. H. A. Clayton, “AB-plot assisted determination of fluorophore mixtures in a fluorescence lifetime microscope using spectra or quenchers,” J. Microscopy **218,** 62-67 (2005).
17. D. A. Jeong, G. Markle, F. Owen, A. Pease and R. Von Bünau Grenville, “The future of optical lithography,” Solid State Technol. **37,** 39-47 (1994).
18. M. D. Levenson, “Extending optical lithography to the gigabit era,” Solid State Technol. 38, 57-66 (1995).
19. L. Geppert, “Semiconductor lithography for the next millennium,” IEEE Spectrum **33**, 33-38 (1996).
20. S. Okazaki, “Resolution limits of optical lithography,” J. Vac. Sci. Technol. B **9,** 2829-2833 (1991).
21. LK van Geest and KWJ Stoop, “FLIM on a wide field fluorescence microscope,” Lett. Peptide Sci. **10,** 501-510 (2003).
22. Robert M. Clegg, Thomas M. Jovin Theodorus and W J Gadella Jr, "Fluorescence lifetime imaging microscopy: Pixel-by-pixel analysis of phase-modulation data," Bioimaging **2,** 139-159 (1994).
23. J.M. Harris and F.E. Lytle, “Measurement of subnanosecond fluorescence decays by sampled single-photon detection,” Rev. Sci. Instrum. **48,** 1470-1476 (1977).
24. Q. S. Hanley, V. Subramaniam and D. J. Arndt-Jovin , "Fluorescence lifetime imaging: multi-point calibration, minimum resolvable differences, and artifact suppression," Cytometry **43,** 248-260 (2001).
25. A. Squire and P.I.H. Bastiaens, "Three dimensional image restoration in fluorescence lifetime imaging microscopy," J. Mircoscopy **193,** 36-49 (1999).
26. M.J. Cole, J. Siegel, S.E.D. Webb, R. Jones, K. Dowling, P.M.W. French, M.J. Lever, L.O.D. Sucharov, M.A.A. Neil, R. Juskaitis and T. Wilson, "Whole-field optically sectioned fluorescence lifetime imaging," Opt. Lett. **25,** 1361-1363 (2000).
27. A.Elder, J. Frank, J. Swartling, X. Dai and C.F. Kaminski, “Calibration of a wide-field frequency-domain fluorescence lifetime microscopy system using light emitting diodes as light sources,” J. Microscopy 2006 (accepted for publication).
28. A. C. Mitchell, J. E. Wall and J. G. Murray, "Direct modulation of the effective sensitivity of a CCD detector: a new approach to time-resolved fluorescence imaging," J. Microsc. Oxf. **206,** 225-232 (2002).

1. Introduction

Microfluidic devices represent an excellent platform to implement a large number of chemical processing and sensing applications [1-7]. Their benefits derive from the fact that timescales for mixing, heating and flow manipulation are much reduced compared to macroscopic flow systems. Furthermore the small size means that little reagent consumption is required and integration with other technologies is readily achieved. A key factor in the usefulness of microfluidics is the availability of matching online diagnostic systems that permit as much physical and chemical information to be sampled as possible. Such analytical techniques require species selectivity, sensitivity, and a high spatial and temporal resolution to be useful for online process monitoring, sensing applications, and product characterisation inside microfluidic channels.

Optical techniques are very powerful in this context and in the past techniques have focused on fluorescence microscopy [8], light microscopy [9], confocal laser scanning microscopy [10], and optical coherence tomography [11]. Of these, fluorescence based techniques are among the most versatile and certainly they are the most widely employed analytical tools in this context. Fluorescence imaging offers information on spatial and temporal scales of concentration, and is easy to implement. There are drawbacks however, relating to signal quantification, which is affected by the presence of local quencher species and also by signal reabsorption. Furthermore there is a requirement for the analyte to have clearly distinguishable absorption and emission spectra. Often this requires elaborate labelling techniques for one to obtain specificity and / or sensitivity - something that is not always a feasible option. In multicomponent mixtures, spectral overlap may cause ambiguity preventing a discrimination of the different components. In such situations the fluorescence lifetime of a sample may give additional or superior information.

The fluorescence lifetime represents the average time a fluorophore will remain in an excited state upon absorption of light before emitting a fluorescence photon. It is a sensitive indicator of a molecule’s interaction with its immediate environment: The presence of local quencher species, pH mediated conformation changes, molecular association and aggregation, diffusional mobilities, etc. all affect the fluorescence lifetime and its measurement thus provides information beyond that of purely intensity based diagnostic techniques.

#69207 - $15.00 USD Received 7 April 2006; revised 26 May 2006; accepted 26 May 2006

Furthermore, components whose spectral signatures are too similar to permit their discrimination can often be differentiated according to their lifetime differences. There is thus a strong case to be made to combine the benefits of fluorescence lifetime imaging with microfluidic device applications. To date, however, there have been very few reported applications of FLIM (fluorescence lifetime imaging microscopy) to microfluidic devices [12,13]. Benninger *et al*. recently reported on the use of two photon excited time resolved Fluorescence Anisotropy and lifetime imaging in microfluidic devices to demonstrate its use for the study of molecular mixing and rotational diffusion effects in microfluidic channels. The system employed an Ar ion pumped Ti:Sapphire laser and an ultrafast image intensification device to achieve time resolution and the usefulness of lifetime resolved imaging was clearly demonstrated. Magennis *et al*. used a similar system comprising of a gated intensified CCD camera and an ultrafast pulsed laser to investigate diffusional mixing.

In this paper we report the application of a novel, Frequency Domain Lifetime Imaging system to microfluidic imaging employing inexpensive incoherent LED sources for excitation, whose intensity is modulated at high frequency (40 MHz). Using a gain modulated wide field detection system in a scheme analogous to homodyne detection, the fluorescence lifetime of the sample can be deduced from the phase shift (and demodulation) of the signal with respect to the excitation waveform [14,15]. The fluorescence lifetime deduced is a single exponential approximation to the true lifetime decay, which for many biological systems may be multi-exponential in nature. Multi-exponential lifetimes can be deduced by taking measurements at several different modulation frequencies and fitting a multi-exponential model to the data, or in special cases by use of techniques such as AB-plot analysis [16]. The system has great potential for miniaturisation and integration with microfluidic technology in a "lab on chip" approach and permits accurate lifetime differences at 100 ps and below to be clearly resolved. We demonstrate quantitative use of the system by imaging the lifetime changes of Rhodamine 6G fluorescent dye (which has a single exponential decay) in a dual inlet microreactor as iodide ions diffuse across two parallel aqueous streams.

2. Material and methods

2.1 Microfluidic device fabrication

A microchannel stamp as detailed in Fig. 1, was fabricated on cleaned wafers using standard photolithographic techniques [17,18,19,20]. This stamp was then used to create a microchannel structure in Poly Dimethylsiloxane (PDMS) using soft lithography techniques (Fig. 2). This fabrication method is extremely flexible with respect to channel design whilst also allowing repeated use of the same stamp. Additionally PDMS was noted as a suitable substrate for the channel fabrication as no background fluorescence was observed during the studies described at the wavelengths used.

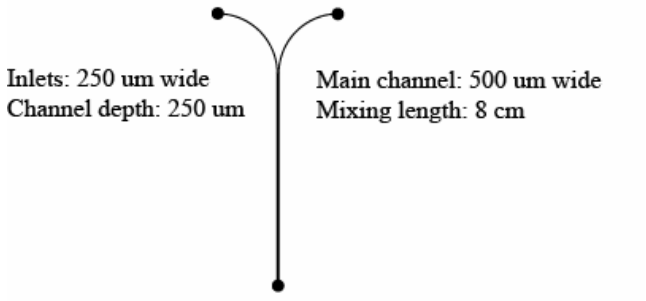

Fig. 1. Design of the dual-inlet stamp used to create PDMS microchannel structure.

#69207 - $15.00 USD Received 7 April 2006; revised 26 May 2006; accepted 26 May 2006

The process involved use of a technical drawing software package to create a high resolution acetate mask of the microchannel design (printed by Circuit Graphics, Chelmsford). Thin films of approximately 250μm Microchem SU8-2100 (Microchem) were coated over the glass wafers using a spin coater (Karl Suss Delta 10) and were pre-baked at 65°C for 12 minutes and 95°C for 60 minutes. The acetate mask was used to project an ultraviolet (UV) light source (340nm) from a mask aligner (Karl Suss MJB3) onto the substrates coated with the film of photoresist. The exposed films of photoresist were then post baked at 65°C and 95°C for 1 minute and 21 minutes respectively, before revealing the photoresist pattern using a developer solution (EC Solvent, Microchem). PDMS (Sylgard 184, Dow Corning) was then poured over the SU-8 master and allowed to cure. Once hardened, the PDMS was peeled off of the master, inlets and outlet attached and sealed onto a clean glass wafer using the natural adhesivesness of the PDMS to create a seal. Figure 2 illustrates the steps involved in fabricating the photoresist pattern.

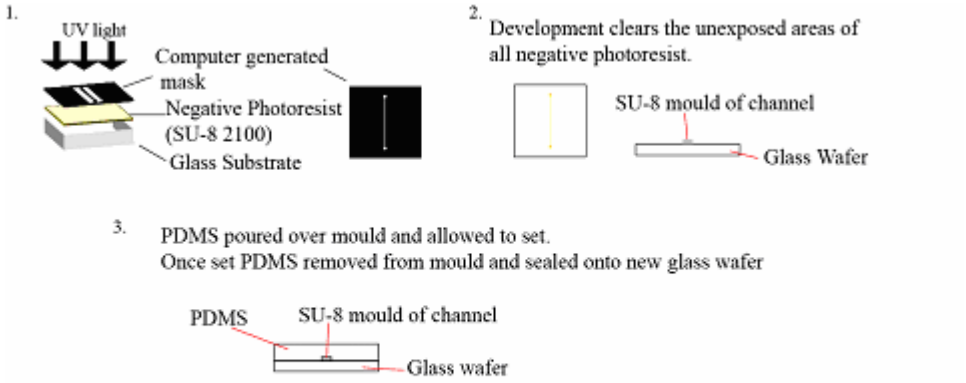

Fig. 2. Microfabrication of dual inlet channel using photolithography and soft lithography.

2.2 FLIM system

The FLIM system (LIFA, Lambert Instruments, Leutingewolde, The Netherlands) [21] was attached to an Olympus IX70 inverted microscope (Olympus UK Ltd, Southall, UK). The excitation light is provided by a high power LED (3W) which can be modulated at frequencies up to 40 MHz. Images are detected by an ICCD whose gain is modulated at the same frequency. To obtain a lifetime image a series of intensity images are acquired at different detector gain phase offsets (typically 8 – 12 steps). The demodulation and phase shift of the fluorescence light are a function of the lifetime and can be determined over the entire field of view by fitting a sine function to every pixel along the set of images [22]. The absolute phase of the system is determined by taking a reference measurement of a standard with a known lifetime.

For Rhodamine 6G measurements we used an LED centred at 473 nm. The excitation light was filtered by a 470 – 490 nm bandpass filter and the emitted fluorescence light was filtered by a 500 nm cut-off dichroic mirror and a 515 nm longpass filter. A 20×, NA=0.70 objective was used for the imaging. The setup allows lifetime images to be acquired in approximately 1 second.

#69207 - $15.00 USD Received 7 April 2006; revised 26 May 2006; accepted 26 May 2006

2.3 FLIM data analysis

All data analysis was performed using software written by the authors in IDL 6.1 (Interactive Data Language, Research Systems, Inc., Boulder, CO). Lifetimes can be determined from either the modulation depth *m* or the phase shift ϕ, referred to as modulation (τ_m) and phase lifetime (τ_ϕ), respectively. The lifetimes returned are single exponential approximations of the true fluorescence lifetimes. In the case of a single exponential decay (as for Rhodamine 6G) the phase and modulation lifetimes are identical. For a multi-exponential decay the phase lifetime will be shorter than the modulation lifetime. With a modulation frequency *f* the modulation lifetime is given by

$$\tau_m = \frac{1}{2\pi f}\sqrt{\frac{1}{m^2}-1} \tag{1}$$

and the phase lifetime by

$$\tau_\phi = \frac{\tan\phi}{2\pi f} \tag{2}$$

To account for the phase shift and demodulation introduced by the electronics and optics it is usually necessary to perform measurements relative to a reference sample with a known fluorescence lifetime, τ_{ref}, using the following equations:

$$\tau_\phi = \frac{1}{2\pi f}\tan\left((\phi-\phi_{ref})+\tan^{-1}(2\pi f\tau_{ref})\right) \tag{3}$$

$$\tau_m = \frac{1}{2\pi f}\left(\frac{m_{ref}^2}{m^2}(1+(2\pi f)^2\tau_{ref}^2)-1\right)^{1/2} \tag{4}$$

where ϕ_{ref}, m_{ref} and τ_{ref} refer to the phase shift, demodulation and lifetime of the reference respectively.

The optimal frequency in terms of lifetime selectivity can be derived from Equations 1 and 2 by differentiation. This results in optimal frequencies $f_{opt,\phi} = 1/(2\pi\tau)$ for the phase lifetime and $f_{opt,m} = \sqrt{2}/(2\pi\tau)$ for the modulation lifetime.

The modulation bandwidths of the LEDs used here is limited to around 40 MHz. This is far from ideal for the shortest lifetimes we observe here (0.5 ns) especially for determinations of τ_m. Demodulations may to levels of a percent or so, making τ_m measurements susceptible to noise and baseline drifts. Determination of phase lifetimes, however, remains relatively

#69207 - $15.00 USD Received 7 April 2006; revised 26 May 2006; accepted 26 May 2006

robust at theses frequencies and as a consequence all data presented here is from phase lifetimes.

2.4 Rhodamine 6G solutions and flow set-up

Iodide quenching of Rhodamine 6G has been used as a convenient method of producing mono-exponential decay standards with variable lifetimes [23,24]. This quenching process follows a Stern-Vollmer model, in which the observed lifetime τ is given by

$$\frac{1}{\tau} = k_q[Q] + \frac{1}{\tau^0} \tag{5}$$

where τ^0 is the lifetime of Rhodamine 6G in the absence of quencher, [*Q*] is the concentration of the quencher, and k_q is the bimolecular reaction rate constant for the reaction of the excited state with the quencher *Q*. Previously reported values for Rhodamine 6G are approximately τ^0 = 4.1 ns.

Rhodamine 6G was first prepared as a stock solution in methanol. This was added to a 0.2 M solution of potassium chloride (KCl) to a dye concentration of 1 μM. A solution of 0.05 M KI and 0.15 M KCl was prepared to be used as the quenching agent. Solutions containing 0.1 M KI and 0.1 M KCl, 0.03 M KI and 0.17 M KCl, 0.005 M KI and 0.195 M KCl were also prepared in order to calibrate the bimolecular reaction rate constant.

Flow in the microchannel device was controlled by a syringe pump (Harvard apparatus, PHD 2000), and was approximately 10μl/min.

In order to examine the flow pattern the channel was imaged just after the inlets using a confocal microscope (Olympus FV300, Olympus UK Ltd, Southall, UK) by taking a stack of images from the top to the bottom of the channel (Fig. 3). In order to clearly distinguish the two parallel streams both contained 0.2M KCl solutions but the dye, Rhodamine 6G, was only present in one.

#69207 - $15.00 USD Received 7 April 2006; revised 26 May 2006; accepted 26 May 2006

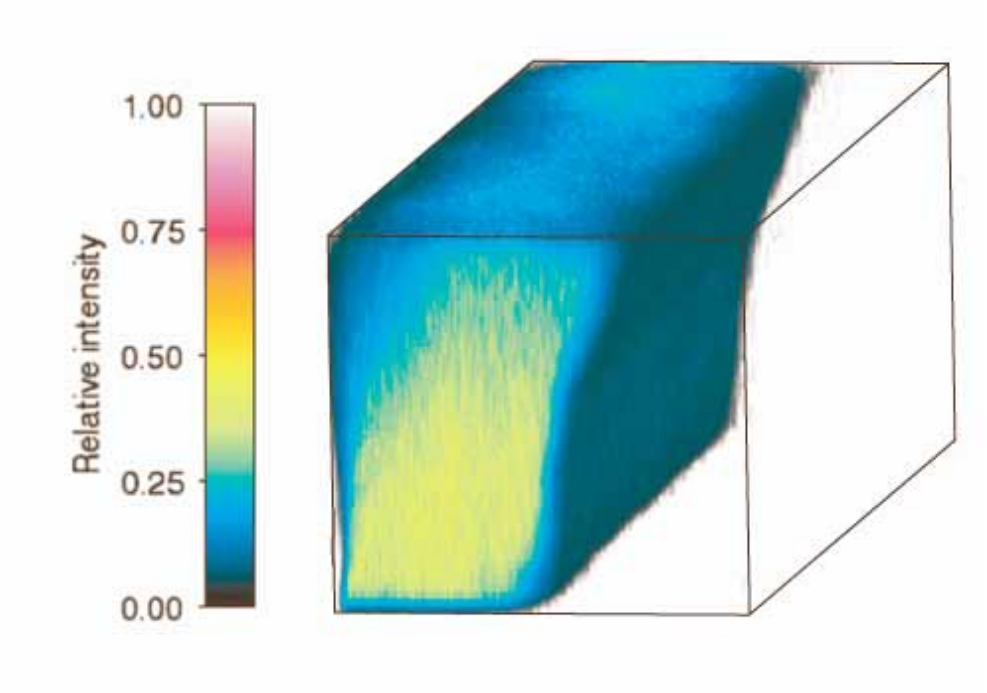

Fig. 3. Confocal 3D image of two parallel aqueous streams flowing down a microchannel, just after the inlets. Only the left flow contained fluorescent dye. The signals seen on the right define the channel wall and stem from residual dye attached to the wall from previous experiments. The loss of fluorescence intensity in the upper part of the channel is due to reabsorption and optical distortion near the walls. The wider profile of the upper part of the fluorescent stream is due to small imperfections in the geometry of the microchannel and its inlets.

3. Results

We used the Rhodamine 6G solution without quencher as the reference standard to calibrate the FLIM system and assumed a lifetime of 4.08 ns [24].

In order to determine the bimolecular reaction rate constant the lifetimes of solutions with different iodide concentrations were imaged in a black well plate. Figure 4 shows a plot of measured lifetime times KI concentration against lifetime. Theory predicts a linear relationship with gradient $-k_q \tau^0$ and intercept τ^0. From the graph we determine the bimolecular reaction rate constant to be 6.64×10^9 dm^3 $mole^{-1}$ s^{-1}.

#69207 - $15.00 USD Received 7 April 2006; revised 26 May 2006; accepted 26 May 2006

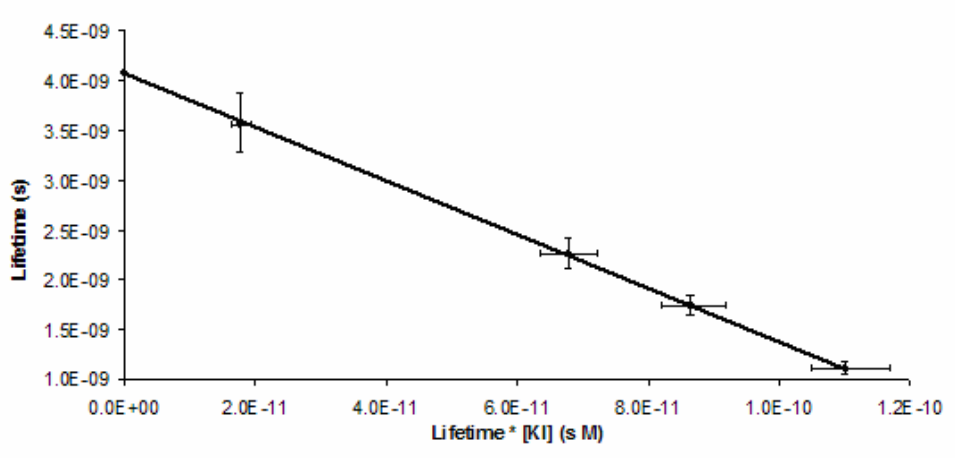

Fig. 4. Calibration plot to determine the Stern-Vollmer quenching parameters for Rhodamine 6G solutions with KI. Each solution contains a different concentration of KI, but the same ionic strength through addition of KCl. From the gradient and intercept the bimolecular reaction rate constant, k_q, is found to be 6.64×10^9 dm^3 $mole^{-1}$ s^{-1}.

Lifetime images taken at increasing distances along the length of the channel are presented in Fig. 5. Profiles of the lifetime and calculated iodide concentration perpendicular to the flow direction for increasing distances down the channel are shown in Fig. 6.

#69207 - $15.00 USD Received 7 April 2006; revised 26 May 2006; accepted 26 May 2006

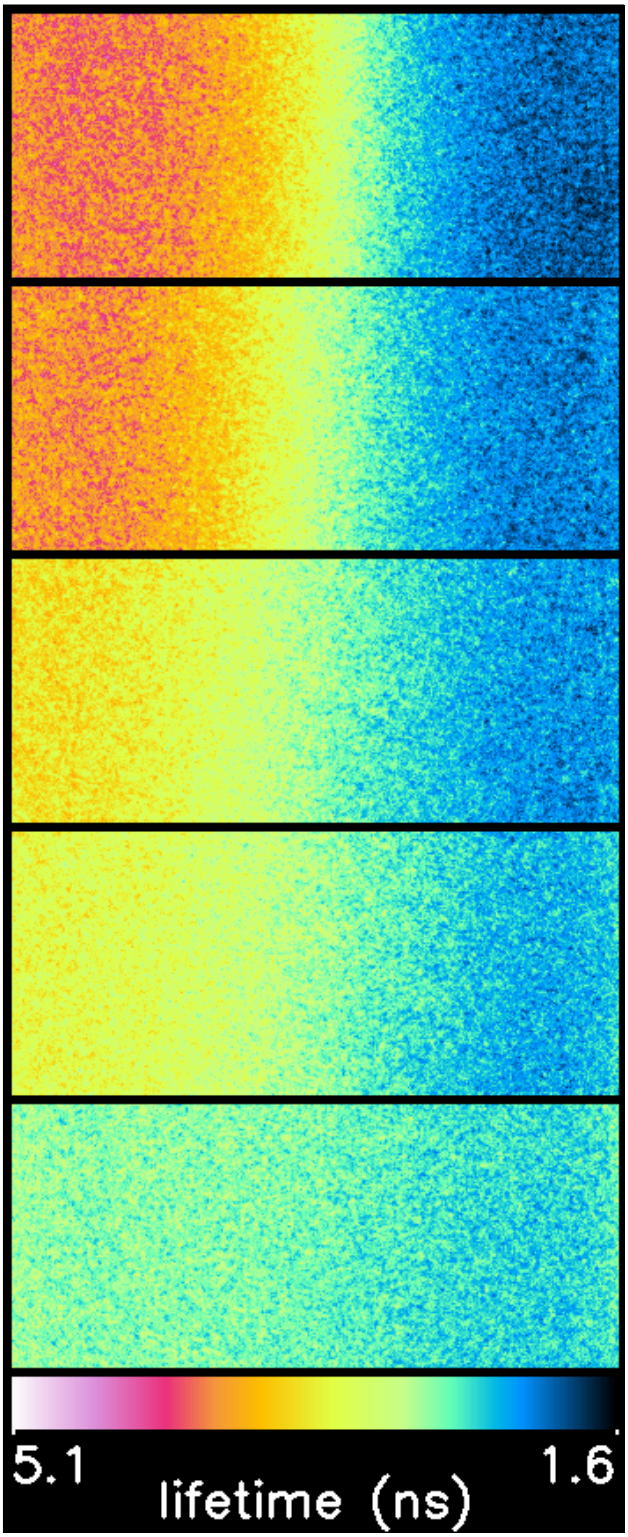

Fig. 5. Lifetime images taken at increasing distances along the length of the channel. The increasing degree of mixing with increasing distance is clearly seen.

#69207 - $15.00 USD Received 7 April 2006; revised 26 May 2006; accepted 26 May 2006

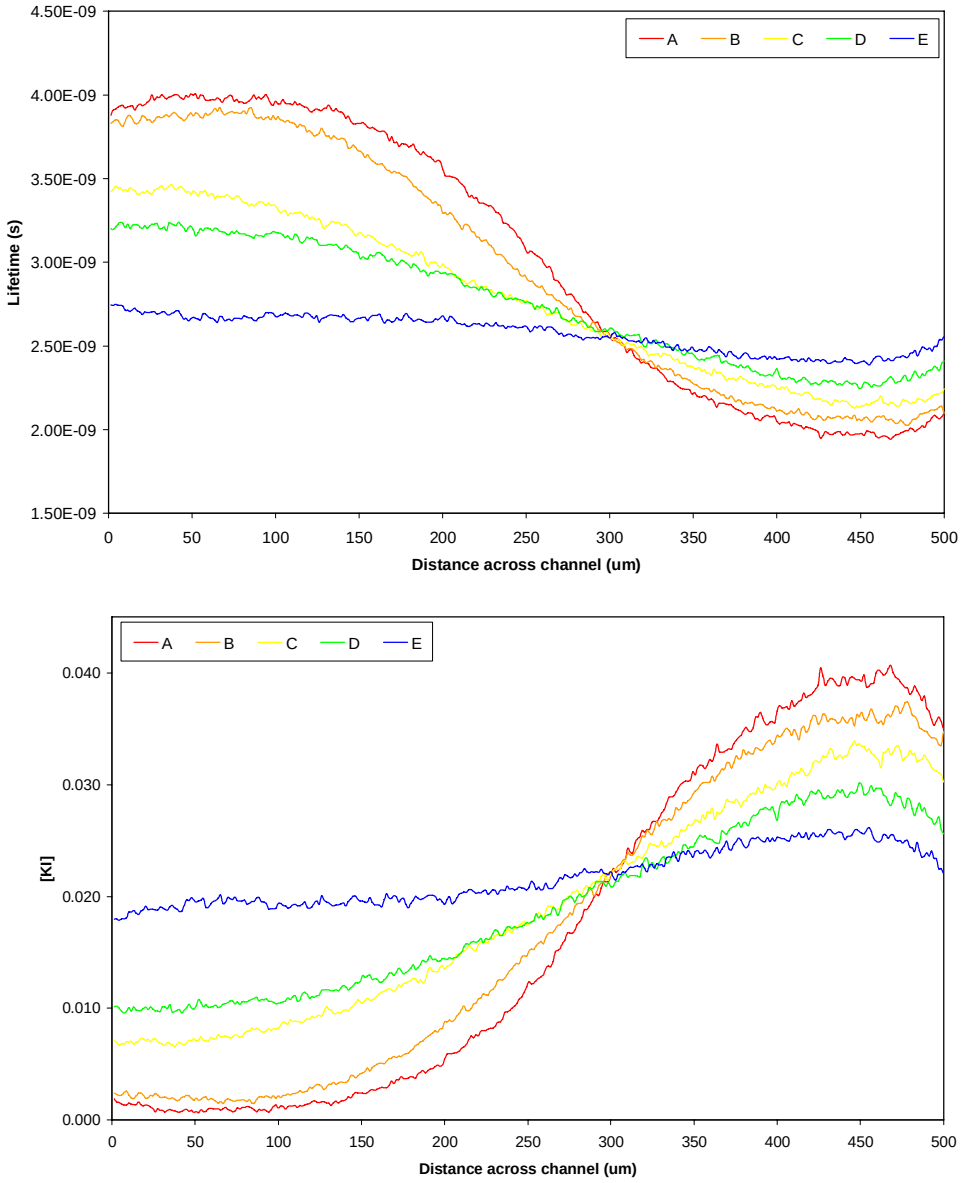

Fig. 6. (a) Plot of lifetime profiles perpendicular to the flow direction for 5 different distances down the channel. Initially one sees a sharper gradient, which gradually becomes less distinct. (b) Concentration profiles derived from the lifetime data according to Equation 3.

4. Discussion

The 3D images from the confocal microscope show a very clear and sharp interface between the two flows just after the inlets which is in agreement with what one would expect from a highly laminar flow (Fig. 3). This confirms that the microchannel device is very well suited for studies of molecular mixing by diffusion across the flow boundary. The confocal images point to the problems associated with fluorescence intensity imaging: variations in the images occur due to absorption of the excitation light, reabsorption of the fluorescence light, and

#69207 - $15.00 USD Received 7 April 2006; revised 26 May 2006; accepted 26 May 2006

optical distortions when imaging deep into the channel. The optical distortions are the result of either spherical or chromatic aberrations caused by focussing using a thicker effective coverslip (required to seal the channel) than the objective was designed for, or a combination of both. All these issues complicate quantitative evaluation of intensity images.

The lifetime images initially show a sharp concentration gradient between the two streams (Fig. 5). As the distance down the channel is increased, the diffusion gradient becomes less well defined, as one would expect from diffusional mixing (Fig. 6). Of particular note is the point where all the lines intersect – at a distance of approximately 290 microns across the channel and at a concentration of 0.021 M KI. The concentration of 0.021 M KI represents the final uniform concentration that the channel will eventually reach. The distance of 290 microns across the channel represents the interface between the two streams, and from its position we can infer the relative flowrates of each stream. By comparing the relative flow rate in each stream multiplied by its initial KI concentration $\left(\left(0.0\times\frac{290}{500}\right)+\left(0.05\times\frac{500-290}{500}\right)=0.021\right)$ with the final 'mixed' concentration (0.021) we see very good agreement.

In Fig. 6 the concentration of KI does not reach the maximum of 0.05 M. We believe that this is because of the lack of *z* (depth) resolution in the images. This means that out of focus light, from a slower moving part of the flow is collected. Because the flow is slower, there has been more time for diffusion and so the KI concentration is reduced. Because the KI concentration is lower, the signal is not only from a higher lifetime but it is also of a brighter intensity, which weights the lifetime signal more in favour of the longer lifetime.

The advantage of lifetime data is clear when considering quantitative interpretation of the results, in our case determination of the concentration of iodide by means of Eqn. 3, owing to the direct relationship between lifetime and concentration. For high resolution 3D mapping of the concentration higher z-resolution would be advantageous. This can be achieved by wide-field optical sectioning techniques, either by means of deconvolution techniques [25] or by the use of structured illumination [26]. Present work is focussed on implementing wide-field optical sectioning on our FLIM set up.

For our system the minimum detectable lifetime difference between a small region of 100 pixels and a large region was evaluated from simulations and found to be around 100 ps when imaging with a SNR (signal-to-noise ratio) of 50 and taking measurements at 12 phase steps [27]. The simulations were performed by generating intensity images corresponding to assumed lifetime distributions and then adding normally distributed noise with a SNR of 50 to the data for every pixel and every phase step. This level of minimum detectable lifetime difference corresponds well with the level of noise seen in the channel profiles in Fig. 6. In the KI concentration region most sensitive to lifetime changes such a change in lifetime would be equivalent to a concentration change of approximately 0.001 M. This illustrates the potential sensitivity of lifetime measurements.

The FLIM system conveniently covers the entire visible spectrum with the use of inexpensive, easily interchangable LEDs. This is in contrast to previous implementations of FLIM systems which have utilised expensive and complex pulsed laser systems or high-frequency optical modulators. The use of low cost LEDs opens the gate for widespread use of FLIM as an analytical tool, and provides the potential for integration in "lab-on-a-chip" type devices. A further development that would again reduces the potential cost of FLIM technology is the use of unintensified rapid-modulation gain camera systems [28].

5. Conclusion

To summarise, we have demonstrated the usefulness of frequency domain FLIM for the study of flows in microchannels by imaging changes in lifetime of Rhodamine 6G due to the diffusion of iodide ions. Changes in fluorescence lifetime profiles were seen as a function of distance along the channel. The lifetime images provide excellent contrast between the two

#69207 - $15.00 USD Received 7 April 2006; revised 26 May 2006; accepted 26 May 2006

parallel flows and permit detailed studies of molecular mixing to be performed. We found that contrast is obtained in situations where intensity based measurements lack specificity and sensitivity and thus the work shown provides an alternative and complementary diagnostic for the study of such systems. The results were obtained with a high power diode as illumination source, the intensity of which was modulated at up to 40 MHz. The work shows that sensitive lifetime information on a microscopic scale is obtainable with such devices and the technology is cost effective and simple to implement.

Acknowledgments

Clemens Kaminski gratefully acknowledges support from the Leverhulme Trust, UK.

Jonathan Frank and Clemens Kaminski gratefully acknowledge support for this work by EPSRC via a PLATFORM grant (GR/R98679/01). Jonathan Frank acknowledges support from the U.S. Department of Energy, Office of Basic Energy Sciences, Division of Chemical Sciences, Geosciences, and Biosciences.

This work was supported by grants received from the Royal Society, Syngenta Ltd, the EPSRC (Engineering and Physical Sciences Research Council, UK), and HEFCE (The Higher Education Funding Council for England, UK).

#69207 - $15.00 USD Received 7 April 2006; revised 26 May 2006; accepted 26 May 2006